Synergistic flame retardant coatings for carbon fibre-reinforced polyamide 6 composites based on expandable graphite, red phosphorus, and magnesium oxide

Zsófia Kovács [a,b], Andrea Toldy [a,b,*]

[a] *Department of Polymer Engineering, Faculty of Mechanical Engineering, Budapest University of Technology and Economics, Műegyetem rkp. 3., Budapest H-1111, Hungary*
[b] *MTA-BME Lendület Sustainable Polymers Research Group, Műegyetem rkp. 3., Budapest H-1111, Hungary*

ARTICLE INFO

ABSTRACT

Continuous fibre-reinforced polyamide 6 (PA6) composites are predominantly prepared by anionic ring-opening polymerisation of low viscosity ε-caprolactam monomer. PA6 melts easily when exposed to flames, which can lead to rapid fire spread due to dripping. For this reason, the use of flame retardants is necessary. We investigated the effects of magnesium oxide (MgO), red phosphorus (RP), and expandable graphite (EG) on the glass transition temperature, crystalline fraction, and thermal stability of PA6. After investigating the flammability properties, we selected the best compositions (MgO and RP combined with EG) and applied them as coatings on carbon fibre-reinforced polyamide 6 composites. A synergistic effect was achieved when RP or MgO were used together with expandable graphite. The 0.5 mm thick coating containing 5% RP and 5% EG reduced the peak heat release rate (pHRR) of the composite by 21% and the total heat release (THR) by 28%, while 5% MgO and 5% EGES100 reduced the pHRR by 27% and the THR by 37%.

1. Introduction

The application of polymer composites in both civil and military applications has become increasingly important. Besides their excellent mechanical properties, the main reason for their widespread use is their high strength-to-weight ratio [1–3]. The matrix material of the traditional continuous fibre-reinforced composites is a thermoset resin, but they have the disadvantage of being difficult to recycle. However, in the context of sustainable development and the impact of waste on the environment, there is now a growing demand for more easily recyclable thermoplastic matrix composites [4–6]. One possible way of producing continuous fibre-reinforced thermoplastic matrix composites is reactive processing, where a low-viscosity monomer or oligomer is injected into the reinforcing material, and polymerisation occurs between the reinforcing materials. In-situ polymerisation requires a monomer with which it is possible to produce a high molecular weight polymer with an adequately high conversion without by-product formation [7]. An important representative of thermoplastic composites is polyamide 6 (PA6), which can be produced by anionic ring-opening polymerisation of low-viscosity (~10 mPa·s) ε-caprolactam (CL) in the presence of an activator and initiator [8–10].

Polyamides might be considered self-extinguishing because of their nitrogen content, but they melt easily in flames, causing dripping and rapid fire spread. However, safety regulations do not permit the use of virgin PA6 in certain high risk applications, necessitating the addition of flame retardants [11–13]. A significant drawback of anionic ring-opening polymerisation is that many factors, such as additives and moisture, can inhibit polymerisation [14,15]. Thus, many flame retardants are not suitable for use in the polymerisation of CL. In the literature [16,17], promising results have been obtained using a phosphorus-containing hexaphenoxycyclotriphosphazene flame retardant with a heterocyclic structure, where access to the P atom is sterically hindered and, therefore, it does not significantly interfere with the polymerisation reaction of CL. Furthermore, the flammability of CL-based PA6 can be significantly reduced by using red phosphorus, magnesium oxide, the polyhalogenated cyclopentadiene derivative (Dechlorane Plus), and a combination of these [18]. Different flame retardancy solutions have been developed for PA6 through the use of in situ water catalysed anionic ring-opening polymerization systems [19–22]. However, it must be mentioned that these systems have a
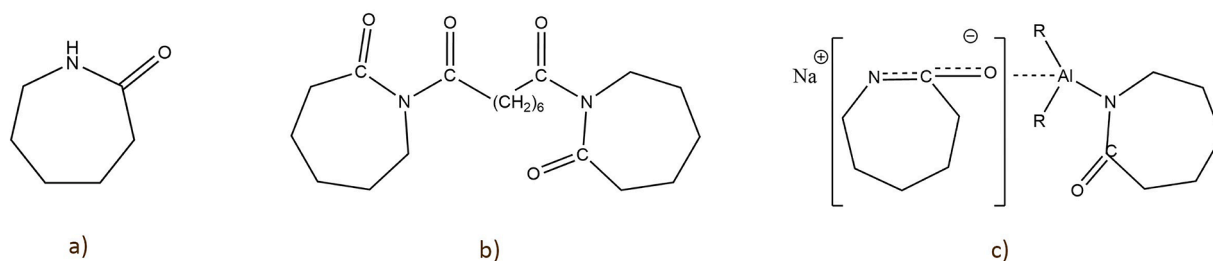
Fig. 1. Chemical structure of ε-caprolactam a), C20 activator b), Dilactamate initiator c).

longer polymerisation time and are therefore unsuitable for thermoplastic resin transfer moulding (T-RTM) [11]. Another problem in the flame retardancy of composites is that reinforcing materials can filter out solid particulate flame retardants, this means that there will be no additives inside the composite. In addition, large amounts of flame retardant additives can degrade the mechanical properties of the composite [23,24]. A solution to these problems is to provide a flame-retardant coating on the surface of the composite. One method of producing coatings is by spraying, but spraying can release large amounts of volatile organic compounds (VOCs) into the air, which are harmful to health. To reduce VOCs, in-mould coating (IMC) can be an effective solution [25]. The problems associated with the flame retardancy of CL-based PA6 and the possible manufacturing technologies have been described in detail in our previous review article [11].

The main objective of our research is to create a flame retardant system that does not hinder the anionic ring-opening polymerisation of ε-caprolactam and effectively reduces the flammability of PA6. In our work, we investigated the effect of flame retardants on the glass transition temperature, crystalline fraction, thermal stability, and flammability. The best-performing compositions were applied to the surface of carbon fibre-reinforced PA6 composites by IMC.

2. Materials and methods

2.1. Materials

AP-NYLON Caprolactam type ε-caprolactam was used as a monomer (CL, L. Brüggemann GmbH & Co. KG, Heilbronn, Germany). We selected *Bruggolen C20P* type hexamethylene-1,6-dicarbamoyl caprolactam (C20, L. Brüggemann GmbH & Co. KG, Heilbronn, Germany) as an activator, which is one of the most commonly used activators, and sodium dicaprolactamato-bis-(2-methoxyethoxo)-aluminate, with a brand name of *Dilactamate* (DL), produced by Katchem (Prague, Czech Republic), as an initiator. DL is less sensitive to moisture, so it can also be appropriately used for hygroscopic additives without a nitrogen atmosphere [11]. CL and C20 were kept under vacuum at 40 °C before use. The chemical structure of CL, C20, and DL are shown in Fig. 1. The flame retardants used were *Exolit RP 607* type red phosphorus (RP, Clariant, Muttenz, Switzerland) with a phosphorus content >95%, magnesium oxide (MgO, Sigma Aldrich, Budapest, Hungary), and two variants of expandable graphite (Graphit Kropfmühl, Hauzenberg, Germany). The difference between the two expandable graphites is in their grain size and the rate of expansion: for expandable graphite *ES100 C10* (EG ES100) type, the grain size is in 75% < 150 μm and the expansion rate is 100 cm^3/g, while for the expandable graphite *ES350 F* (EG ES350) type, the grain size is in 80% > 300 μm and the expansion rate is 350 cm^3/g. The flame retardants were dried at 80 °C for 4 h before use. Unidirectional carbon fibre reinforcement (CF, trade name: PX 35 UD 300, aerial weight: 333 g/m^2) by Zoltek Ltd., Nyergesújfalu, Hungary) was used as composite reinforcement.

2.2. Preparation of flame retardant PA6 coating materials

In the first step, the effect of flame retardants on the thermal properties and flammability of PA6 was investigated. For this purpose, samples of PA6 without reinforcing materials were prepared (Chapter 2.2), and only the best-performing formulations were applied as coatings (Chapter 2.4) on PA6 composites (Chapter 2.3). The reference ε-caprolactam-based PA6 was prepared using 87 mass% CL, 3 mass% C20, and 10 mass% DL. For the flame retarded samples, we tried to find a balance between mechanical properties and flame retardant properties when selecting the optimum amount, so we added 10 mass% of flame retardant to the caprolactam system in all cases. According to the article [18], above 10 mass% of flame retardant, the polymerisation time increases and conversion yield decreases. An aluminium mould was used as a simplified, small-scale version of thermoplastic resin transfer moulding (T-RTM) and preheated in a 150 °C oven. The measured monomer and activator, and in the case of flame retarded samples, the flame retardant, were mixed and melted at 120 °C using an MR Hei-TEC type (Heidolph, Germany) heated magnetic stirrer. After adding the initiator, test specimens were prepared according to standard flammability tests (100 × 100 × 4 mm^3 for mass loss type cone calorimetric measurements and 120 × 10 × 4 mm^3 for UL-94 tests and limiting oxygen index measurements).

2.3. Preparation of CF/PA6 composites

A 100 × 100 × 2 mm^3 mould was used to produce the composites. Five layers of unidirectional CF reinforcement were placed in the mould in [0]$_5$ layer order. The closed mould containing the reinforcing material was preheated in a drying oven at 150 °C. The CL-based PA6 matrix was prepared using 87 mass% CL, 3 mass% C20, and 10 mass% DL. The ε-caprolactam and the activator were melted at 120 °C and mixed with an MR Hei-TEC type (Heidolph, Germany) magnetic stirrer. After adding the initiator, the melt was injected into the closed mould using a Hamilton syringe (1025 TLL 25 ml SYR) to ensure adequate pressure, and the mould was removed from the drying chamber after 15 min. With this process, composites with 50 mass% fibre content were produced.

2.4. Preparation of flame retardant coating for CF/PA6 composites

An aluminium mould with a cavity of 100 × 100 × 2.5 mm^3 was used to model the IMC. The composite was pre-placed in the mould. After closing the mould, it was preheated in a drying oven at 150 °C. To produce the 0.5 mm coating, CL was melted in the presence of an activator and flame retardant at 120 °C using an MR Hei-TEC type (Heidolph, Germany) heated magnetic stirrer, and after the addition of the initiator, the melted ε-caprolactam system was introduced into the closed mould using a Hamilton syringe, and the mould was removed from the drying chamber after 15 min.

2.5. Characterisation

The glass transition temperatures and the crystalline fraction of the

Table 1
The results of DSC for reference and flame retarded PA6 samples (T_g: glass transition temperature; ΔH_m: enthalpy of crystallisation for the first heating; ΔH_c: enthalpy of crystallisation; X_c: crystalline fraction; Average standard deviation of the temperature measurements: $\pm$ 0.5 °C).

Sample	T_g [°C]	ΔH_m [J/g]	ΔH_c [J/g]	X_c [%]
PA6	49	78.6	45.9	42
PA6/10%RP	49	75.4	47.1	45
PA6/10%MgO	44	73.2	42.6	43
PA6/10%EGES100	46	66.7	32.9	39
PA6/10%EGES350	47	92.9	45.6	55
PA6/5%RP/5%MgO	49	76.7	46.6	45
PA6/5%RP/5%EGES100	50	80.7	35.6	48
PA6/5%RP/5%EGES350	47	80.1	50.2	47
PA6/5%MgO/5%EGES100	46	95.0	46.3	56
PA6/5%MgO/5%EGES350	51	95.4	38.6	56

Table 2
The results of TGA for flame retardant and reference PA6 samples ($T_{-5\%}$: the temperature at 5% mass loss; $T_{-50\%}$: the temperature at 50% mass loss; dTG_{max}: maximum mass loss rate; T_{dTGmax}: temperature belonging to the maximum mass loss rate; Average standard deviation values: temperature measurements: $\pm$ 0.5 °C, mass measurements: $\pm$ 1%).

Sample	$T_{-5\%}$ [°C]	$T_{-50\%}$ [°C]	dTG_{max} [%/°C]	T_{dTGmax} [°C]	Char yield at 600 °C [%]
PA6	241	341	2.1	338	2.0
PA6/10%RP	332	439	1.5	432	35.0
PA6/10%MgO	215	404	1.8	422	10.7
PA6/10%EGES100	243	446	1.0	437	38.6
PA6/10%EGES350	152	435	1.0	439	27.1
PA6/5%RP/5%MgO	123	383	0.9	435	7.4
PA6/5%RP/5% EGES100	220	422	1.0	445	10.1
PA6/5%RP/5% EGES350	214	425	1.0	442	11.4
PA6/5%MgO/5% EGES100	247	382	1.4	402	9.3
PA6/5%MgO/5% EGES350	142	357	0.9	396	10.8

Table 3
The results of UL-94 and LOI for reference and flame retardant coating materials (Average standard deviation of the LOI: $\pm$1 vol%).

Sample	UL-94 ranking	LOI [%]
PA6	HB	21
PA6/10%RP	HB	26
PA6/10%MgO	HB	21
PA6/10%EGES100	HB	25
PA6/10%EGES350	V-1	25
PA6/5%RP/5%MgO	V-2	25
PA6/5%RP/5%EGES100	V-0	26
PA6/5%RP/5%EGES350	V-1	25
PA6/5%MgO/5%EGES100	HB	24
PA6/5%MgO/5%EGES350	HB	24

reference and flame retarded PA6 samples were measured using a TA Instruments Q2000 (New Castle, DE, USA) differential scanning calorimeter (DSC). Samples of 2–5 mg were analysed in a 50 ml/min N_2 flow. Heating-cooling-heating cycle measurements were performed at 25–250 °C. The heating and cooling rate was 10 °C/min.

Thermogravimetric analysis (TGA) was used to study thermal stability and monomer conversion. TA Instruments Q500 (New Castle, DE, USA) device was used for the test, with a 30 ml/min flow rate under a N_2 atmosphere at a heating rate of 20 °C/min between 30–600 °C. 2–5 mg of samples were used in the tests.

In UL-94 flammability testing (ISO 9772, ISO 9773), the flame spread rate was determined in the horizontal arrangement (H-type) and the flammability classification in the vertical arrangement (V-type).

We performed oxygen index tests (LOI) according to ISO 4589–1 and ISO 4589–2 standards. The oxygen index is the minimum oxygen content by volume of an oxygen-nitrogen gas mixture flowing at a specified velocity in the test sample that is still burning.

Mass loss type cone calorimetry (MLC, Fire Testing Technology, East Grinstead, UK) was used to determine the complex combustion characteristics of the samples. Samples with a surface area of 100×100 mm^2 were subjected to a heat flux of 50 kW/m^2. A spark ignition unit assisted in the ignition of the specimen surfaces. The time to ignition (TTI), total heat release (THR), peak heat release rate (pHRR), time to pHRR, total burn time, and residual mass were determined.

The flammability of the coatings was also investigated by pyrolysis combustion flow calorimetry (PCFC, Fire Testing Technology, East Grinstead, UK). The measurement was performed according to ASTM D-7309 at a heating rate of 1 °C/s on 8–10 mg samples. The maximum pyrolysis temperature was 750 °C, and the combustion temperature was 900 °C. The flow rate of nitrogen was 80 ml/min, and the flow rate of oxygen was 20 ml/min.

The combustion residue of the reference and combustion inhibited samples was examined using a JEOL JSM 6380LA scanning electron microscope (SEM, Jeol Ltd., Tokyo, Japan). The samples were coated with gold using a Jeol JPC1200 cathodic sputtering gold plating apparatus.

3. Results and discussion

In the initial phase of our study, we examined the coatings themselves and assessed the samples containing 10% flame retardants, both as standalone additives and as mixed formulations. We investigated the effect of the flame retardants on the glass transition temperature (T_g), crystalline fraction, thermal stability, and flammability of PA6. The best compositions in flammability were applied as flame retardant coatings on the surface of carbon fibre-reinforced PA6 composites.

3.1. Characterisation of PA6 coating materials

3.1.1. Glass transition temperature and crystallinity of flame retardant PA6 coating materials

The effect of the flame retardants on the glass transition temperature and the crystalline fraction was investigated by differential scanning calorimetry. The results of the DSC measurements are shown in Table 1. The first and second heating curves and the cooling curves are presented in the Appendix (Figure A.1).

The crystalline fraction (X_c) was determined from the enthalpy of crystal melting (ΔH_m) of the first heating curve using the following relation:

$$X_c = \frac{\Delta H_m}{\Delta H_{100\%}(1-\alpha)} \cdot 100 \tag{1}$$

where α is the filler content of the sample, $\Delta H_{100\%}$ is the enthalpy change associated with the theoretical 100% crystalline melting of the sample, which for PA6 is $\Delta H_{100\%}$=188 J/g [26].

The DSC measurements showed that the flame retardants did not significantly affect the glass transition temperature; in most cases, it was between 45–50 °C. The crystalline fraction ranged from 39% to 56%, with the highest crystalline fraction for samples containing 5%MgO/5% EGES100 and 5%MgO/5%EGES350. It can be said that the effect of the flame retardants increased the crystalline fraction except for the PA6/10%EGES100 sample.

3.1.2. Thermal stability of flame retardant PA6 coating materials

The thermal stability of PA6 with different flame retardants was investigated by TGA. Table 2 shows the results of the TGA measurements of flame retardant PA6 samples, including the temperature
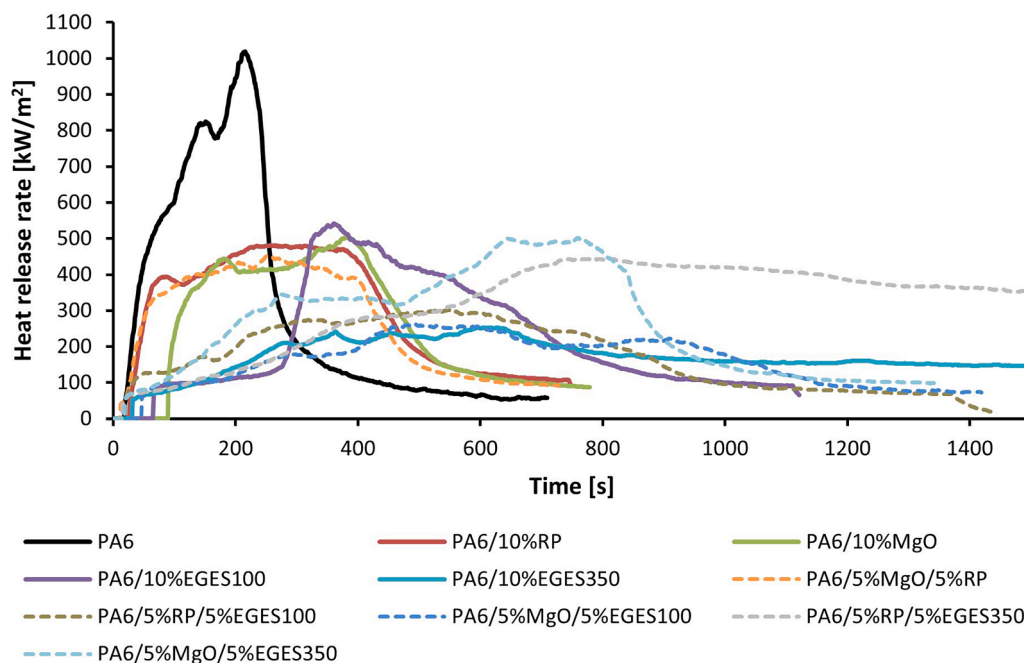
Fig. 2. The heat release rate of reference and flame-retarded polyamide 6 samples measured by MLC (mixed compositions are marked with a dashed line).

Table 4
The results of MLC for reference and flame retardant polyamide 6 samples (TTI: time to ignition, pHRR: peak heat release rate, THR: total heat release, MARHE: maximum average rate of heat emission, EHC: effective heat of combustion, FRI: flame retardancy index, Average standard deviation of the measured mass loss calorimeter values: TTI: ±3; pHRR: ±30; time to pHRR: ±5; residue: ±2).

Sample	TTI [s]	pHRR [kW/m^2]	time to pHRR [s]	THR [MJ/m^2]	MARHE [kW/m^2]	EHC [MJ/kg]	Residue [%]	FRI [-]
PA6	19	1019	218	213	8.8	40.3	1.5	–
PA6/10%RP	27	481	266	219	5.8	35.3	3.9	2.9
PA6/10%MgO	90	504	383	196	2.8	32.8	10.6	10.4
PA6/10%EGES100	66	541	360	244	1.5	40.6	6.6	5.7
PA6/10%EGES350	33	253	596	232	1.6	64.2	32.5	6.4
PA6/5%RP/5%MgO	12	454	253	197	5.6	34.7	7.6	1.5
PA6/5%RP/5%EGES100	18	301	547	243	3.1	43.5	10.9	2.8
PA6/5%RP/5%EGES350	16	445	808	420	3.2	110.5	20.8	1
PA6/5%MgO/5%EGES100	47	265	492	219	1.4	40.3	7.7	9.3
PA6/5%MgO/5%EGES350	19	502	761	349	2.8	62.7	7	1.2

corresponding to 5% and 50% mass loss (T$_{-5\%}$ and T$_{-50\%}$), the maximum mass loss rate (dTG$_{max}$) and the corresponding temperature (T$_{dTGmax}$), and the char yield at 600 °C. The TGA and DTG curves are presented in the appendix (Figure A.2).

The T$_{-5\%}$ was higher than the reference only in the case of samples containing 10% RP alone, 10% EGES100 alone, 5% MgO and 5% EGES100 in combination. The reference sample reached 50% mass loss at 341 °C. The increased values of T$_{-50\%}$ (even up to 446 °C in the case of EGES100) in flame retarded samples indicate the improvement in thermal stability due to the flame retardants. Only the samples containing MgO exhibited values lower than 400 °C but still at least 16 °C higher (PA6/5%MgO/5%EGES350) than in the case of the reference PA6. The T$_{dTGmax}$ also increased above 400 °C (except for sample PA6/5%MgO/5%EGES350), and the dTG$_{max}$ decreased. The residual mass shows a significant increase compared to the reference. For samples containing red phosphorus and expandable graphite, the values for T$_{-50\%}$ were above 420 °C, and the T$_{dTGmax}$ values were above 440 °C, while for the samples containing only expandable graphite, these values were all above 430 °C. In the mixed samples, there is no significant difference in the residual mass depending on the grain size of the graphite used. The sample with the highest residual mass (38.6%) was PA6/10%EGES100.

3.1.3. Flame retardancy of PA6 coating materials

The flammability of PA6 coatings was analysed by UL-94 testing, LOI, MLC and PCFC. The results of the UL-94 test and LOI are shown in Table 3.

PA6 without flame retardants exhibited an oxygen index of 21% and obtained an HB rating in UL-94 testing. When introducing standalone flame retardants (except for MgO), the LOI increased by as much as 5% by volume, as observed in the PA6/10%RP sample. All mixed-composition flame retardants increased the LOI. Notably, in the case of PA6/5%RP/5%EGES100, the LOI reached a maximum of 26%. In the UL-94 test, only this composition attained a V-0, self-extinguishing rating. The literature [27] suggests a synergistic effect when RP and EG are used together. The addition of RP increases the mass of the char and makes the residue more stable. This is particularly important as EG itself exhibits ash flying behaviour, easily disintegrating under external influence. Due to the more stable char formed, heat and mass transfer from combustion can be more effectively prevented.

The MLC test curves are shown in Fig. 2, and the values obtained are summarised in Table 4.

In the MLC tests, the reference sample ignited the fastest (19 s). With the addition of flame retardants, the ignition time can be shifted by up to 71 s. The flame retardants reduced the pHRR value compared to the
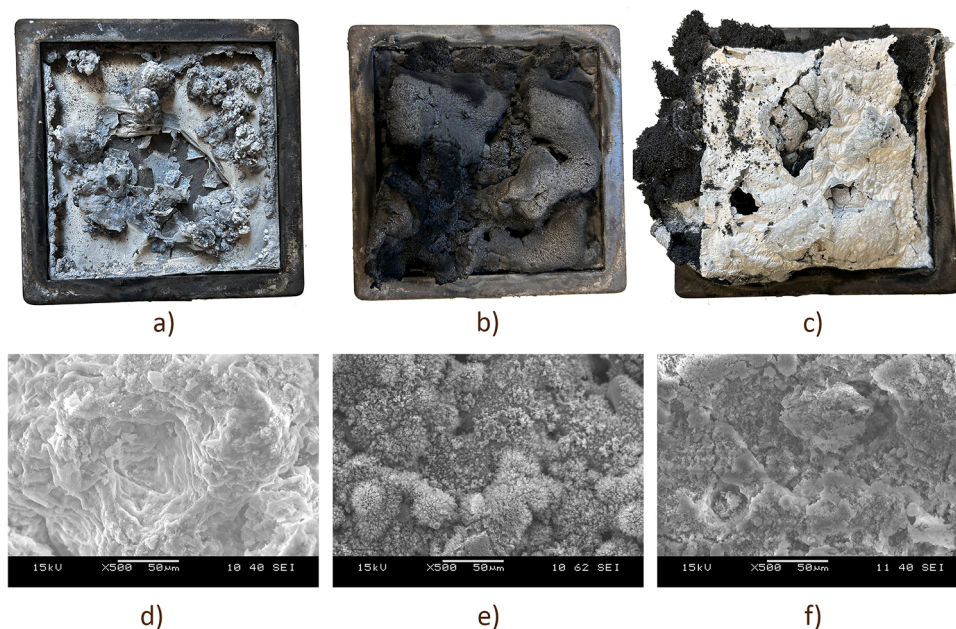
Fig. 3. Residue after combustion for PA6 a), PA6/5%RP/5%EGES100 b), PA6/5%MgO/5%EGES100 c) samples and SEM image of samples PA6 d), PA6/5%RP/5% EGES100 e), PA6/5%MgO/5%EGES100 f).
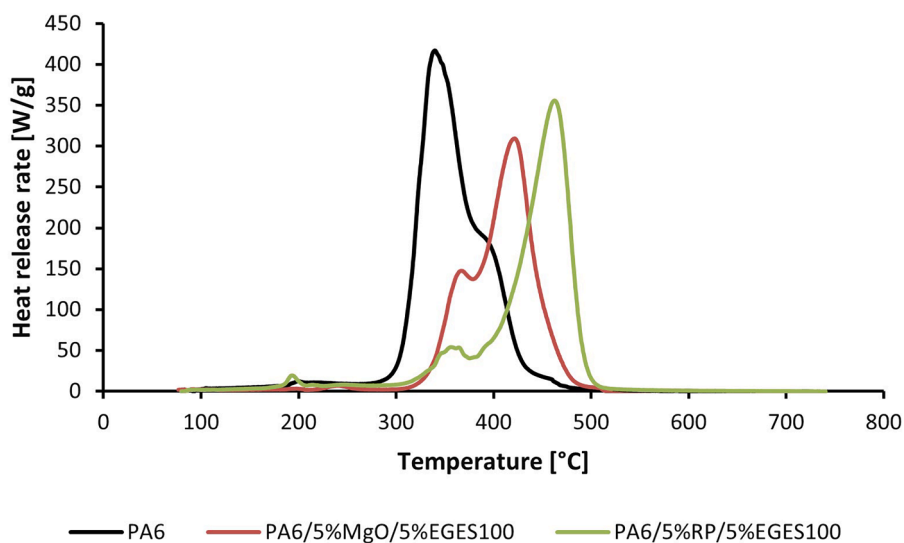
Fig. 4. The heat release rate of reference and flame-retarded polyamide 6 samples measured by PCFC.

Table 5
The results of PCFC for reference and flame retardant coating materials (pHRR: peak heat release rate, T_{pHRR}: temperature of pHRR, THR: total heat release).

Sample	pHRR [W/g]	time to pHRR [s]	T_{pHRR} [°C]	THR [kJ/g]	Residue [%]
PA6	416	343	340	28	1.7
PA6/5%MgO/5% EGES100	309	440	421	22	16.1
PA6/5%RP/5% EGES100	355	510	463	22	9.7

reference, and the lowest pHRR was obtained with 10% EGES350. Expandable graphite is a flame retardant acting in the condensed phase; thus, it creates a charred protective layer on the sample surface during combustion. This also increases the mass remaining after combustion

(32.5%). The residual mass of MLC samples due to incomplete pyrolysis and charring may be higher than the residual mass measured in the TGA test (complete pyrolysis with charring). This can be observed for samples containing 5%RP/5%EGES100, 5%RP/5%EGES350, 5%RP/5%MgO and 10%EG350. The mixed composition of flame retardants did not significantly increase the ignition time, but the time to pHRR was delayed by up to 590 s. For the samples containing EG ES350, the time to maximum heat release increased by almost four times compared to the reference. The worm-like formations that formed during the intense swelling process reached the heating wire in the conical heater of the calorimeter. The heat release curves did not decay due to the heat release and high temperature provided by the heating filament. As a result, the THR values for samples with RP and EGES350 were distorted, and the results were not as expected. When RP and MgO were used together with expandable graphite, the pHRR was significantly reduced. The reduction can be explained by the combined use of flame retardants
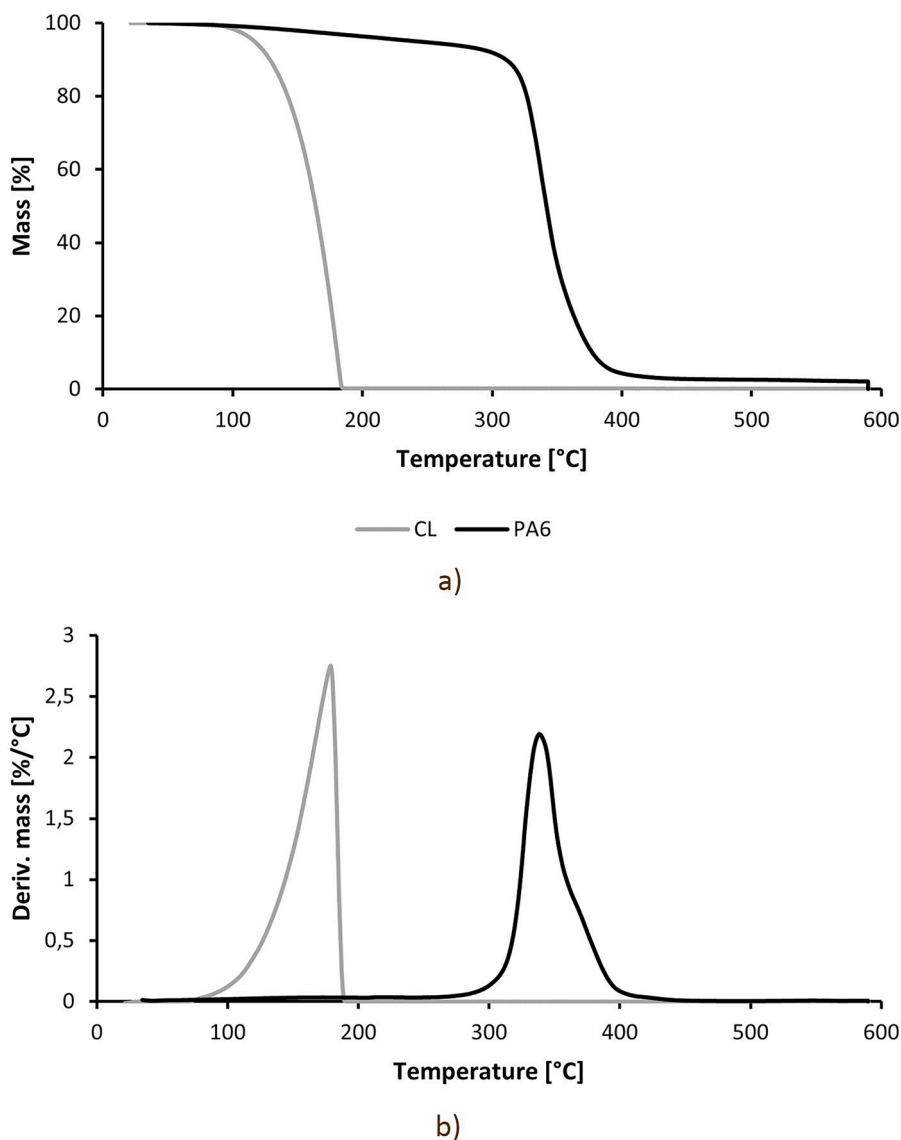
Fig. 5. TGA a) and DTG b) curves of ε-caprolactam and polyamide 6.

Table 6
The results of TGA for ε-caprolactam, PA6, and flame retardants (T$_{-5\%}$: the temperature at 5% mass loss; T$_{-50\%}$: the temperature at 50% mass loss; dTG$_{max}$: maximum mass loss rate; T$_{dTGmax}$: temperature belonging to the maximum mass loss rate); Average standard deviation values: temperature measurements: ± 0.5 °C, mass measurements: ± 1%).

Sample	T$_{-5\%}$ [°C]	T$_{-50\%}$ [°C]	dTG$_{max}$ [%/°C]	T$_{dTGmax}$ [°C]	Char yield at 600 °C [%]
CL	117	164	2.8	179	0.1
PA6	241	341	2.1	338	2.0
RP	417	483	1.5	496	13.0
MgO	328	–	0.1	338	91.8
EGES100	228	–	0.4	228	75.7

with different mode of action. In the case of MgO, the FR catalyses thermal-oxidative degradation, accelerating the formation of a barrier at the surface. In addition, MgO reduces the activation energies and accelerates the evolution of incombustible CO_2 in the initial degradation stage, which is favourable for improving the flame retardancy; and improves thermal stability at the end of the degradation process [28]. The fire retardant properties of EG are attributed to the formation of a dense charcoal layer due to its expansion. This expansion is the result of a redox process between H_2SO_4 incorporated between the graphite layers and the graphite itself. This reaction generates blowing gases which, when heated above 200 °C, cause a significant increase in the volume of the materials. The expansion of the graphite forms a structure similar to a "worm" which effectively suffocates the flame. In addition, the dense char layer limits the transfer of heat and mass from the material to the heat source, thus inhibiting further decomposition of the polymer [29–31]. By combining EG with MgO, the thickness of the char layer can be increased [32]. RP mainly acts in the condensed phase [33, 34], however, in addition to the condense phase mode of action, the gas phase mode of action also exists [29,35]. When RP is oxidised in the condensed phase, phosphorus oxide is created. This oxide can then react with water resulting from the degradation of the material to produce phosphoric acid or polyphosphoric acid, which covers the surface of the polymer. Additionally, according to a radical trapping mechanism, RP can function as a flame retardant in the gas phase by generating PO free radicals, which can eliminate H and OH of flame [36]. When RP and expandable graphite are combined, after ignition, the expandable graphite forms a char layer with poor thermal conductivity [37], which protects the substrate from further thermal effects. In addition, as the temperature increases, the phosphorus starts to oxidise, and various
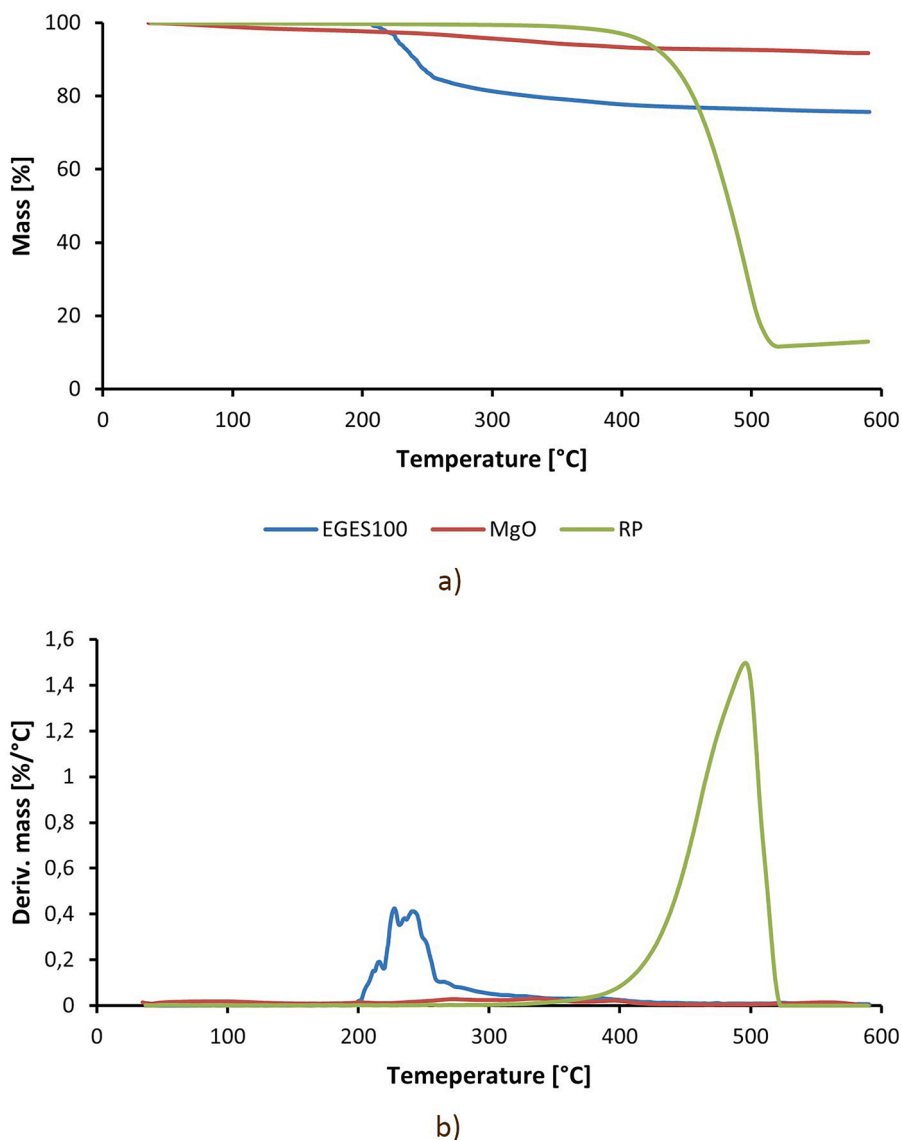
Fig. 6. TGA a) and DTG b) curves of the flame retardants.

P-containing groups form, which can react further with the graphite in the char layer under the influence of oxygen and heat, resulting in a more stable protective char layer [38]. The synergistic action of RP and MgO can result in a higher yield of phosphoric acid and, thus, a higher rate of char formation on the polymer surface [18,39].

We also examined the maximum average rate of heat emission (MARHE) values, which showed that in all cases, compared to the 8.8 kW/m^2 obtained for the reference PA6, the MARHE was reduced by the effect of the flame retardants. The lowest MARHE value was obtained for PA6/5%MgO/5%EGES100 (1.4 kW/m^2), which is 84% lower than the reference. The effective heat combustion (EHC) value was lower than the reference (40.3 MJ/kg) only for samples containing 10% RP, 10% MgO and 5% RP/5% MgO. It can be said that samples containing EGES350 show a significant increase compared to the reference. This can be explained by the distorted THR values.

The Flame Retardancy Index (FRI) was calculated using the following formula:

$$FRI = \frac{\left(\frac{THR \cdot pHRR}{TTI}\right)_{reference}}{\left(\frac{THR \cdot pHRR}{TTI}\right)_{modified}} \qquad (2)$$

where THR [MJ/m^2] is the total heat release, pHRR [kW/m^2] is the peak heat release rate, and TTI [s] is the time to ignition.

The FRI is a dimensionless parameter widely used in the literature [40] to compare flame retarded and reference polymers. By calculating the FRI, flame retarded polymers can be characterised as follows: if FRI<1, the flame retardancy is poor; if 1<FRI<10, the flame retardancy is good; if 10<FRI, the flame retardancy is excellent. The FRI values were used for relative comparison only, and the value of the flame retarded samples was compared to the reference. The FRI values show that the flame retardant effect is excellent for the PA6/10%MgO sample, but the other flame retardants and their combinations resulted in a good flame retardancy level as well. Based on the comparison of the relative values, the sample with the lowest FRI was PA6/5%RP/5%EGES350, which could be explained by the fact that the thermal emission of the heating wire during the intensive foaming process could have distorted the THR value.

Based on the flammability tests, the sample containing 10% EGES350 lead to the lowest pHRR when used as the sole additive. However, due to the large particle size of the expandable graphite, significant sedimentation was observed in the samples. Before the polymerisation was completed, the expandable graphite accumulated in
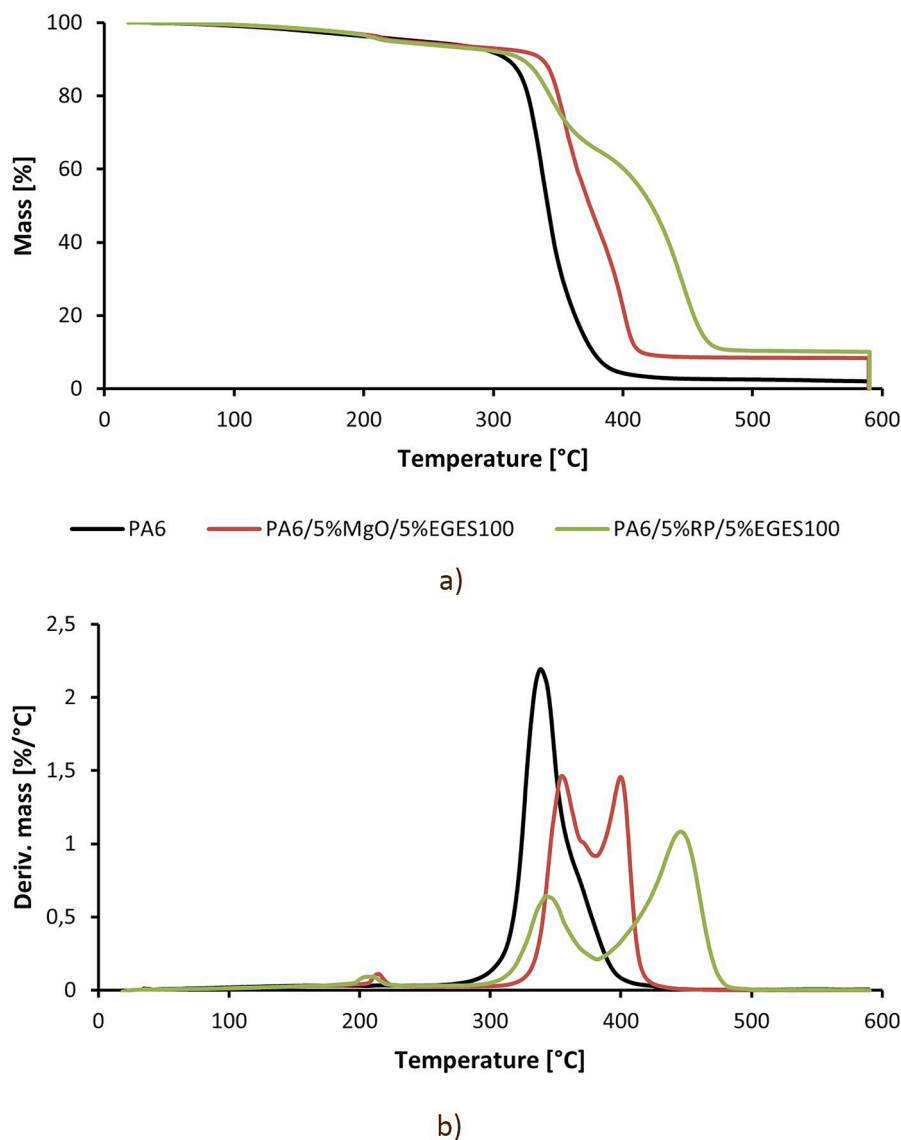
Fig. 7. TGA a) and DTG b) curves of reference and flame-retarded polyamide 6.

Table 7
The results of MLC for reference and flame retardant composites (TTI: time to ignition, pHRR: peak heat release rate, THR: total heat release, Average standard deviation of the measured mass loss calorimeter values: TTI: ±3; pHRR: ±30; time to pHRR: ±5; residue: ±2).

Sample	TTI [s]	pHRR [kW/ m²]	time to pHRR [s]	THR [MJ/ m²]	Residue [%]
PA6/CF	17	346.7	164	95.3	32.5
PA6/CF/5%MgO/5% EGES100	21	252.3	65	68.3	40.7
PA6/CF/5%RP/5% EGES100	24	273.9	62	59.5	44.2

the lower part of the mould, resulting in an uneven distribution. For this reason, samples containing large grains of expandable graphite were not tested further. Therefore, the two selected flame retardant compositions are the following:

- 5%MgO/5%EGES100
- 5%RP/5%EGES100

Images of the residues of the reference sample and the selected compositions after combustion, and their SEM images, are shown in Fig. 3.

It can be seen from the combustion residues that no coherent protective layer was formed on the PA6 reference material, and the aluminium sample holder was also burnt out due to the high heat emission. In contrast, a coherent layer was formed on the surface of the residue of the samples containing mixed composition flame retardants. In both flame retarded samples, a more porous layer was formed inside the residue, where worm-like structures can be observed, typical of expandable graphite. The SEM images for the flame retarded samples were taken from the outer part of the residue.

The flammability of the reference and the selected flame retardant compositions was also tested with PCFC. The results of the test are shown in Fig. 4 and Table 5.

The reference PA6 sample had the highest maximum pHRR, which was reduced by up to 26% by adding MgO and EGES100 flame retardants. The time to pHRR increased by up to 167 s with the combined use of RP and EGES100. The temperature of pHRR shifted by 81 °C for sample PA6/5%MgO/5%EGES100 and 123 °C for sample PA6/5%RP/5%EGES100. The total heat release was reduced by 21% in both mixed formulations. The mass remaining after the test shows a significant
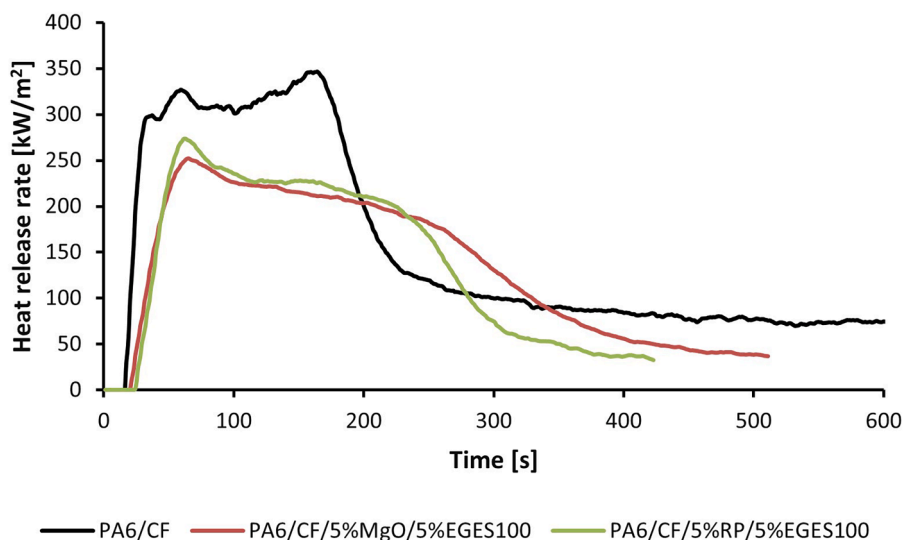
Fig. 8. The heat release rate of reference and polyamide 6 samples with flame retardant coating measured by MLC.

increase compared to the reference, mainly due to EGES100 acting in the condensed phase. In combination with expandable graphite, MgO increases the thickness of the char layer, while RP increases its stability [32,38]. This explains the higher residual of sample PA6/5%MgO/5% EGES100.

3.1.4. Monomer conversion of PA6 coating materials

If the conversion is incomplete, CL monomer may remain in PA6 during anionic ring-opening polymerisation. The residual monomer content is worth investigating as the low molecular weight caprolactam has a plasticising effect and may thus affect the mechanical properties of the final product. The monomer conversion of ε-caprolactam was investigated by TGA. The TGA results of CL monomer and PA6 are shown in Fig. 5 and Table 6.

The decomposition of CL takes place between 100–190 °C. The temperature at 5% mass loss of caprolactam is 117 °C, and the temperature at the maximal decomposition rate is 179 °C. The decomposition of the reference PA6 starts at around 240 °C, where the polymer chain breaks. The temperature at 5% mass loss is 241 °C, and the temperature at the maximal decomposition rate for PA6 is around 340 °C.

For TGA measurements, it is worth paying attention to the overlap of the individual peaks [41]. To investigate whether there is an overlap between the decomposition temperature of the flame retardants and the decomposition temperature of the CL, we investigated the decomposition of the flame retardants (without PA6) by TGA. The TGA results of the flame retardants are presented in Fig. 6 and Table 6.

The results show that the decomposition of expandable graphite starts above 200 °C, with the temperature at the maximal decomposition rate of 228 °C. The TGA studies also provide information on the mode of action of flame retardants. This is particularly true for flame retardants acting in the condensed phase since forming a charred protective layer reduces the mass loss rate. EGES100 is a condensed-phase flame retardant, which can also be seen from the mass loss of the sample, as 71% of the sample mass is retained at 600 °C due to the formation of a charred protective layer. RP decomposed between 350–520 °C, and the temperature at the maximal decomposition rate was 496 °C. RP exerts its effect in both gas and condensed phases. Due to the condensed phase mode of action, it was observed that the flame retardant did not completely decompose at 600 °C, with a residual mass of 12.9%. The MgO was hardly decomposed, with a mass loss of only 9% at 600 °C.

Based on the TGA measurement (Fig. 5), CL decomposition occurs between 100–190 °C. According to the literature [42], above 200 °C, PA6 depolymerises, and the detectable CL is derived from the

decomposition rather than an unreacted residue. Based on these results, the residual monomer content of the flame-retarded samples was investigated between 100–190 °C. Based on the TGA of the flame retardants (Fig. 6), it can be concluded that the decomposition range of the flame retardants does not overlap with the decomposition range of CL. The TGA curves of the reference and the flame retarded PA6 samples are shown in Fig. 7. In the conversion calculation, the amount of the FRs was subtracted from the total mass, and the mass loss was given in terms of pure CL. The results show that the flame retardants did not significantly affect the monomer conversion, with 97.6–97.9% achieved.

3.2. Flame retardancy of CF/PA6 composites with flame retardant coating

The flammability of composites with flame retardant coatings was investigated using MLC. The results of MLC testing of reference and flame retardant-coated PA6 composites are presented in Table 7 and Fig. 8.

The flame retardant coatings significantly reduced the maximum heat release rate of the samples. The lowest maximum heat release was achieved with PA6/CF/5%MgO/5%EGES100, where the pHRR was reduced by 27% compared to the reference. In all the coated samples, an intense increase in heat release is observed until the charred protective layer is formed. As this protective layer thickens, the heat release starts to decrease. The residual mass increased in all samples due to the intense foaming of the expandable graphite and the formation of a charred protective layer. The highest residual mass was obtained for the composite coated with 5% RP and 5% EG ES100. The PA6/CF/5%MgO/5% EGES100 sample has a residual mass of 40.7%, while the PA6/CF/5% RP/5%EGES100 sample has a residual mass of 44.2%. For the composites with coating, the residual mass is lower than the fibre content, which can be explained by the fact that the fibre content was measured on the uncoated composite. For the reference PA6 composite, the residual mass is less than 50%. This can be explained by the fact that the aluminium sample holder is burnt out due to the high heat emission. Even though the mass of the composite was increased by the coating, the total heat release was also reduced by up to 37%. Because of the greater thermal thickness (and thermal inertia) of coated samples, the ignition time is also delayed. Based on the MLC measurements, it can be concluded that the flame retardant coatings can be effectively used to flame retard CL-based PA6 composites.

4. Conclusions

In our research, we first investigated the effects of different flame retardants on the glass transition temperature, crystalline fraction, thermal stability, and flammability of PA6. We used as flame retardants red phosphorus, magnesium oxide, and expandable graphite with two different particle sizes. The flame retardants did not significantly affect the glass transition temperature and the crystalline fraction but improved the thermal stability of PA6. In addition, the flame retardants did not affect the monomer conversion, as 97% conversion was achieved. Combined with expandable graphite; red phosphorus and magnesium oxide reduced the maximum heat release rate of PA6 samples. The flame retardants with different mode of actions had a synergistic effect. The best-performing flame retardant formulations (PA6/5% MgO/5%EGES100, PA6/5%RP/5%EGES100) were applied in 0.5 mm thickness on the surface of carbon fibre-reinforced PA6 composites by in-mould coating. The 0.5 mm thick coating containing 5% MgO and 5% EGES100 reduced the maximum heat release of the composite by 27% compared to the reference. The effect of flame retardants also reduced the total heat release by up to 37%. The expandable graphite acting in the condensed phase, in synergistic combination with red phosphorus or magnesium oxide, formed a stable charred protective layer on the composite after combustion, and significantly increased the residual mass.

CRediT authorship contribution statement

Zsófia Kovács: Writing – review & editing, Writing – original draft, Visualization, Validation, Resources, Investigation, Formal analysis. **Andrea Toldy:** Writing – review & editing, Visualization, Supervision, Resources, Project administration, Methodology, Funding acquisition, Conceptualization.

Declaration of competing interest

The authors declare that they have no known competing financial interests or personal relationships that could have appeared to influence the work reported in this paper.

Data availability

Data will be made available on request.

Acknowledgements

Supplementary materials

Supplementary material associated with this article can be found, in the online version, at doi:10.1016/j.polymdegradstab.2024.110696.

References

[1] Á. Pomázi, A. Toldy, Development of fire retardant epoxy-based gelcoats for carbon fibre reinforced epoxy resin composites, Prog. Org. Coat. 151 (2021) 106015, https://doi.org/10.1016/j.porgcoat.2020.106015.

[2] S. Kuwashiro, N. Nakao, S. Matsuda, T. Kakibe, H. Kishi, Ionic cross-linked methacrylic copolymers for carbon fiber reinforced thermoplastic composites, Express Polym. Lett. 16 (2022) 116–129, https://doi.org/10.3144/expresspolymlett.2022.10.

[3] G. Szebényi, High-performance composites and medical applications of polymers - the sunny side of the polymer industry, Express Polym. Lett. 16 (2022) 1113, https://doi.org/10.3144/expresspolymlett.2022.81. -1113.

[4] M. Valente, I. Rossitti, I. Biblioteca, M. Sambucci, Thermoplastic composite materials approach for more circular components: from monomer to in situ polymerization, a review, J. Compos. Sci. 6 (2022) 132, https://doi.org/10.3390/jcs6050132.

[5] B.M. Campos, S. Bourbigot, G. Fontaine, F. Bonnet, Thermoplastic matrix-based composites produced by resin transfer molding: a review, Polym. Compos. 43 (2022) 2485–2506.

[6] A. Toldy, Challenges and opportunities of polymer recycling in the changing landscape of European legislation, Express Polym. Lett. 17 (2023) 1081, https://doi.org/10.3144/expresspolymlett.2023.81.

[7] N.V. Dencheva, D.M. Vale, Z.Z. Denchev, Dually reinforced all-polyamide laminate composites via microencapsulation strategy, Polym. Eng. Sci. 57 (2016) 806–820, https://doi.org/10.1002/pen.24456.

[8] J. Lee, J.W. Lim, M. Kim, Effect of thermoplastic resin transfer molding process and flame surface treatment on mechanical properties of carbon fiber reinforced polyamide 6 composite, Polym. Compos. 41 (2020) 1190–1202, https://doi.org/10.1002/pc.25445.

[9] J.J. Murray, C. Robert, K. Gleich, E.D. McCarthy, C.M. Ó Brádaigh, Manufacturing of unidirectional stitched glass fabric reinforcedpolyamide 6 by thermoplastic resin transfer moulding, Mater. Des. 189 (2020) 108512, https://doi.org/10.1016/j.matdes.2020.108512.

[10] Z. Osváth, A. Szőke, S. Pásztor, L.B. Závoczki, G. Szarka, B. Iván, Recent advances in the synthesis and analysis of polyamide 6 and products therefrom: from polymerization chemistry of ε-caprolactam to thermoplastic resin transfer molding (T-RTM), Acad. J. Polym. Sci. 4 (2020) 100118, https://doi.org/10.19080/AJOP.2020.04.555629. -0012.

[11] Z. Kovács, Á. Pomázi, A. Toldy, The flame retardancy of polyamide 6—prepared by in situ polymerisation of ε-caprolactam—For T-RTM applications, Polym. Degrad. Stab. 195 (2022) 109797, https://doi.org/10.1016/j.polymdegradstab.2021.109797.

[12] J. Sun, D. Zhang, Y. Yang, Z. Gou, Z. Fang, P. Chen, J. Li, Improving flame retardancy and mechanical properties of polyamide 6 induced by multiple reactions among flame retardants and matrix, React. Funct. Polym. 187 (2023) 105590, https://doi.org/10.1016/j.reactfunctpolym.2023.105590.

[13] W.-J. Jin, Y. Yuan, J.-P. Guan, X.-W. Cheng, G.-Q. Chen, Preparation of durable coating for polyamide 6: analysis the role of DOPO on flame retardancy, anti-dripping and combustion behavior, Polym. Degrad. Stab. 215 (2023) 110418, https://doi.org/10.1016/j.polymdegradstab.2023.110418.

[14] J. Herzog, R. Wendel, P.G. Weidler, M. Wilhem, P. Rosenberg, F. Henning, Moisture adsorption and desorption behavior of raw materials for the T-RTM process, J. Compos. Sci. 5 (2021) 12, https://doi.org/10.3390/jcs5010012.

[15] A.A. Lopez, J. Andres, J.A. Garcia-Manrique, Study of the proper sintering conditions of anionically-polymerized polyamide 6 matrices for the fabrication of greencomposites, Mater. Sci. Forum. 712 (2012) 121–126, https://doi.org/10.4028/www.scientific.net/MSF.713.121.

[16] C.-C. Höhne, R. Wendel, B. Käbisch, T. Anders, Hexaphenoxycyclotriphosphazene as FR for CFR anionic PA6 via T-RTM a study of mechanical and thermal properties, Fire Mater. 41 (2016) 291–306, https://doi.org/10.1002/fam.2375.

[17] C. Yan, P. Yan, H. Xu, D. Liu, G. Chen, G. Cai, Y. Zhu, Preparation of continuous glass fiber/polyamide6 composites containing hexaphenoxycyclotriphosphazene: mechanical properties, thermal stability, and flameretardancy, Polym. Compos. 43 (2021) 1022–1037, https://doi.org/10.1002/pc.26431.

[18] G.C. Alfonso, G. Costa, M. Pasolini, S. Russo, A. Ballistreri, G. Montaudo, C. Puglisi, Flame-resistant polycaproamide by anionic polymerisation of ε-caprolactam in the presence of suitable flame-retardant agents, J. Appl. Polym. Sci. 31 (1986) 1373–1382, https://doi.org/10.1002/app.1986.070310521.

[19] J. Vasiljevic, M. Colovic, I. Jerman, B. Simoncic, A. Demsar, Y. Samaki, M. Sobak, E. Sest, B. Golja, M. Leskovsek, V. Bukosek, J. Medves, M. Barbalini, G. Malucelli, S. Bolka, In situ prepared polyamide 6/DOPO-derivative nanocomposite for melt-spinning of flame retardant textile filaments, Polym. Degrad. Stab. 166 (2019) 50–59, https://doi.org/10.1016/j.polymdegradstab.2019.05.011.

[20] J. Vasiljevic, M. Colovic, N.C. Korosin, M. Sobak, Z. Stirn, I. Jerman, Effect of different flame-retardant bridged DOPO derivatives on properties of in situ produced fiber-forming polyamide 6, Polymers (Basel) 12 (2020) 657, https://doi.org/10.3390/polym12030657.

[21] X. Zhang, L. Sun, Y. Chen, C. Yin, D. Liu, E. Ding, Flame retarded polyamide-6 composites via in situ polymerization of caprolactam with perylene-3,4,9,10-tetracarboxylic dianhydride, SN Appl. Sci. 1 (2019) 1428, https://doi.org/10.1007/s42452-019-1505-1.

[22] K. Liu, Y. Li, L. Tao, C. Liu, R. Xiao, Synthesis and characterization of inherently flame retardant polyamide 6 based on a phosphine oxide derivative, Polym. Degrad. Stab. 163 (2019) 151–160, https://doi.org/10.1016/j.polymdegradstab.2019.03.004.

[23] Á. Pomázi, A. Toldy, Multifunctional gelcoats for fiber reinforced composites, Coatings 9 (2019) 173, https://doi.org/10.3390/coatings9030173.

[24] A. Toldy, Flame retardancy of carbon fibre reinforced composites, Express Polym. Lett. 12 (2018) 186, https://doi.org/10.3144/expresspolymlett.2018.17.

[25] O.V. Semperger, D. Török, A. Suplicz, Development and analysis of an in-mold coating procedure for thermoplastic resin transfer molding to produce PA6 composites with a multifunctional surface, Period. Polytech. Mech. Eng. 66 (2022) 350–360, https://doi.org/10.3311/PPme.21048.

[26] J.E. Mark, Polymer Data Handbook, Oxford University Press, Oxford, 1999.

[27] W. Ji, Y. Yao, J. Guo, B. Fei, X. Gu, H. Li, J. Sun, S. Zhang, Toward an understanding of how red phosphorus and expandable graphite enhance the fire resistance of expandable polystyrene foams, J. Appl. Polym. Sci. 137 (2020) 49045, https://doi.org/10.1002/app.49045.

[28] Q. Dong, C. Gao, Y. Ding, F. Wang, B. Wen, S. Zhang, T. Wang, M. Yang, A polycarbonate/magnesium oxide nanocomposite with high flame retardancy, J. Appl. Polym. Sci. 123 (2012) 1085–1093, https://doi.org/10.1002/app.34574.

[29] M. Modesti, A. Lorenzetti, Halogen-free flame retardants for polymeric foams, Polym. Degrad. Stab. 78 (2002) 167–173, https://doi.org/10.1016/S0141-3910 (02)00130-1.

[30] F. Tomiak, A. Schoeffel, K. Rathberger, D. Drummer, Expandable graphite, aluminum diethylphospinate and melamine polyphosphate as flame retarding system in glass fiber-reinforced PA6, Polymers (Basel) 14 (2022) 1263.

[31] F. Tomiak, K. Rathberger, A. Schöffel, D. Drummer, Expandable graphite for flame retardant PA6 applications, Polymers (Basel) 13 (2021) 2733, https://doi.org/10.3390/polym13162733.

[32] H. Vahabi, A. Raveshtian, M. Fasihi, R. Sonnier, M.R. Saeb, L. Dumazert, B. K. Kandola, Competitiveness and synergy between three flame retardants in poly (ethylene-co-vinyl acetate), Polym. Degrad. Stab. 143 (2017) 164–175, https://doi.org/10.1016/j.polymdegradstab.2017.07.005.

[33] B. Schartel, R. Kunze, D. Neubert, Red phosphorus-controlled decomposition for fire retardant PA 66, J. Appl. Polym. Sci. 83 (2002) 2060–2071, https://doi.org/10.1002/app.10144.

[34] S.V. Levchik, G.F. Levchik, A.I. Balabanovich, G. Camino, L. Costa, Mechanistic study of combustion performance and thermal decomposition behaviour of nylon 6 with added halogen-free fire retardants, Polym. Degrad. Stab. 54 (1996) 217–222, https://doi.org/10.1016/S0141-3910(96)00046-8.

[35] H. Seefeldt, U. Braun, M.H. Wagner, Residue stabilization in the fire retardancy of wood-plastic composites: combination of ammonium polyphosphate, expandable graphite, and red phosphorus, Macro Mol. Chem. Phisics. 213 (2012) 2370–2377, https://doi.org/10.1002/macp.201200119.

[36] N.H. Thi, T.N. Nguyen, H.T. Oanh, N.T.T. Trang, D.Q. Tham, H.T. Nguyen, T. Van Nguyen, M.H. Hoang, Synergistic effects of aluminum hydroxide, red phosphorus, and expandable graphite on the flame retardancy and thermal stability of polyethylene, J. Appl. Polym. Sci. 138 (2020) 50317, https://doi.org/10.1002/app.50317.

[37] F. Meng, P. Amyotte, X. Hou, C. Li, C. He, G. Li, C. Yuan, Y. Liang, Suppression effect of expandable graphite on fire hazard of dust layers, Process Saf. Environ. Prot. 168 (2022) 1120–1130, https://doi.org/10.1016/j.psep.2022.10.063.

[38] N. Wang, L. Li, Y. Xu, K. Zhang, X. Chen, H. Wu, Synergistic effects of red phosphorus masterbatch with expandable graphite on the flammability and thermal stability of polypropylene/thermoplastic polyurethane blends, Polym. Polym. Compos. 28 (2019) 209–219, https://doi.org/10.1177/0967391119869552.

[39] F. Laoutid, L. Ferry, J.M. Lopez-Cuesta, A. Crespy, Flame-retardant action of red phosphorus/magnesium oxide and red phosphorus/iron oxide compositions in recycled PET, Fire Mater. 30 (2006) 343–358, https://doi.org/10.1002/fam.914.

[40] H. Vahabi, B.K. Kandola, M.R. Saeb, Flame retardancy index for thermoplastic composites, Polymers (Basel) 11 (2019) 407, https://doi.org/10.3390/polym11030407.

[41] B. Perret, K.H. Pawlowski, B. Schartel, Fire retardancy mechanisms of arylphosphates in polycarbonate (PC) and PC/acrylonitrile-butadiene-styrene, J. Therm. Anal. Calorim. 97 (2009) 949–958, https://doi.org/10.1007/s10973-009-0379-7.

[42] S. Kurt, J. Maier, R. Horny, S. Horn, D. Koch, J. Moosburger-Will, Determination of the residual monomer concentration of ε-caprolactam in polyamide-6 using thermogravimetric analysis coupled with Fourier transform infrared spectroscopy gas analysis, J. Appl. Polym. Sci. 138 (2021) 50730, https://doi.org/10.1002/app.50730.